

Realistic shell model calculation of  $2\nu\beta\beta$   
nuclear matrix elements  
and role of shell structure in intermediate  
states

H. Nakada

*Department of Physics, Faculty of Science, Chiba University,  
Yayoi-cho 1-33, Inage-ku, Chiba 263, Japan*

T. Sebe

*Department of Applied Physics, College of Engineering, Hosei University,  
Kajino-cho 3-7-2, Koganei, Tokyo 184, Japan*

and

K. Muto

*Department of Physics, Faculty of Science, Tokyo Institute of Technology,  
Oh-okayama 2-12-1, Meguro-ku, Tokyo 152, Japan*

PACS numbers: 23.40.-s, 21.60.Cs, 23.40.Hc

Keywords:  $2\nu\beta\beta$  decay, nuclear matrix element, shell model calculation, shell structure

### Abstract

We discuss two conditions needed for correct computation of  $2\nu\beta\beta$  nuclear matrix-elements within the realistic shell-model framework. An algorithm in which intermediate states are treated based on Whitehead's moment method is inspected, by taking examples of the double  $GT^+$  transitions  $^{36}\text{Ar} \rightarrow ^{36}\text{S}$ ,  $^{54}\text{Fe} \rightarrow ^{54}\text{Cr}$  and  $^{58}\text{Ni} \rightarrow ^{58}\text{Fe}$ . This algorithm yields rapid convergence on the  $2\nu\beta\beta$  matrix-elements, even when neither relevant  $GT^+$  nor  $GT^-$  strength distribution is convergent. A significant role of the shell structure is pointed out, which makes the  $2\nu\beta\beta$  matrix-elements highly dominated by the low-lying intermediate states. Experimental information of the low-lying  $GT^\pm$  strengths is strongly desired. Half-lives of  $T_{1/2}^{2\nu}(\text{EC}/\text{EC}; ^{36}\text{Ar} \rightarrow ^{36}\text{S}) = 1.7 \times 10^{29}\text{yr}$ ,  $T_{1/2}^{2\nu}(\text{EC}/\text{EC}; ^{54}\text{Fe} \rightarrow ^{54}\text{Cr}) = 1.5 \times 10^{27}\text{yr}$ ,  $T_{1/2}^{2\nu}(\text{EC}/\text{EC}; ^{58}\text{Ni} \rightarrow ^{58}\text{Fe}) = 6.1 \times 10^{24}\text{yr}$  and  $T_{1/2}^{2\nu}(\beta^+/\text{EC}; ^{58}\text{Ni} \rightarrow ^{58}\text{Fe}) = 8.6 \times 10^{25}\text{yr}$  are obtained from the present realistic shell-model calculation of the nuclear matrix-elements.

# 1 Introduction

The nuclear double- $\beta$  ( $\beta\beta$ ) decay is a good probe to investigate neutrino masses and some basic properties of the weak interaction[1, 2, 3]. The  $0\nu$  mode, if it exists, immediately indicates a defect of the standard model. On the other hand, the  $2\nu$  mode occurs within the standard model. This mode has a practical importance, because it governs the lifetime of the nuclei which concern  $\beta\beta$  decay. Moreover, the observation of the  $2\nu\beta\beta$  decays[2] has revealed serious discrepancies between earlier predictions and the observed half-lives. It probably originated in a problem of the nuclear structure theories. This problem may be crucial also to the  $0\nu\beta\beta$  decays, because some of the nuclear matrix-elements associated with the  $0\nu$  mode have similarity to the  $2\nu$  mode.

The  $2\nu\beta\beta$  decay takes place by two sequential Gamow-Teller (GT) transitions, via virtual intermediate states. It is not always possible for the current nuclear structure theories to give reliable predictions even on single-GT transitions, since the GT transitions are sensitive to some details of nuclear many-body wavefunctions. The most promising approach to the GT transitions seems to be realistic shell-model calculations. It is yet difficult to apply realistic shell-model approaches to the relatively heavy nuclei where the  $2\nu\beta\beta$  decays have been observed. It may become possible in the near future, however, to carry out a reliable shell-model calculation in a few of these nuclei, with assistance of the growing computer power.

Several realistic shell-model calculations have been reported for the  $^{48}\text{Ca} \rightarrow ^{48}\text{Ti} \beta^-\beta^-$  decay[9, 10, 11], although it has not been observed. In Ref.[9],

it has been pointed out that, among a large number of possible intermediate states, the lowest  $1^+$  state gives a dominant contribution to the  $2\nu\beta\beta$  process. In Ref.[10], a method to handle the intermediate states has been developed based on Whitehead's moment method[12]. Rapid convergence by this method has been shown for the  $^{48}\text{Ca}$  decay. The  $^{48}\text{Ca}$  case is, however, somewhat special, as will be discussed later. It is worth examining generality of these suggestions, by taking other sample nuclei.

While most experimental efforts have been cast on the double- $\beta^-$  ( $\beta^-\beta^-$ ) decays, the  $\beta^+$  side is also important. Since the electron capture (EC) and positron emission ( $\beta^+$ ) are possible in a single-GT $^+$  transition, we have three cases in the double-GT $^+$  transitions; EC/EC,  $\beta^+$ /EC and  $\beta^+\beta^+$ [4, 5]. It has been pointed out that, in the  $0\nu$  mode, they seem to yield quite a different constraint on the neutrino masses and right-handed weak-current parameters[6], although the double-GT $^+$  transitions are more difficult to be observed than the  $\beta^-\beta^-$  cases. From the viewpoint of the nuclear structure theories, there is no essential distinction in the algorithm to compute the  $\beta\beta$  matrix-elements, between the  $\beta^-$  and the  $\beta^+$  cases. In the  $A \lesssim 60$  region, where realistic shell-model wavefunctions are available, the  $\beta^+$  side delivers a few candidates for the  $\beta\beta$  decay in addition to  $^{48}\text{Ca}$ . These candidates give us a good opportunity to test the theoretical methods. One important issue is practical treatment of the intermediate states. Primarily focusing on this point, we shall discuss in this article how to compute the  $2\nu\beta\beta$  nuclear matrix-elements within the realistic shell-model framework, by taking a few sample cases from the  $\beta^+$  side; the  $^{36}\text{Ar} \rightarrow ^{36}\text{S}$ ,  $^{54}\text{Fe} \rightarrow ^{54}\text{Cr}$  and  $^{58}\text{Ni} \rightarrow ^{58}\text{Fe}$  decays, where realistic shell-model wavefunctions are available for the initial

and final states[7, 8]. We will also discuss the key features to describing the  $2\nu\beta\beta$  nuclear matrix-elements.

## 2 Shell model calculation of $2\nu\beta\beta$ matrix elements

In this section, we present a realistic shell-model calculation of the  $2\nu\beta\beta$  nuclear matrix-elements. We discuss the conditions required for treating the intermediate states. The algorithm proposed in Ref.[10] is argued in the light of these conditions, and is re-examined for the examples of the  $^{36}\text{Ar} \rightarrow ^{36}\text{S}$ ,  $^{54}\text{Fe} \rightarrow ^{54}\text{Cr}$  and  $^{58}\text{Ni} \rightarrow ^{58}\text{Fe}$  decays.

With respect to the  $^{36}\text{Ar}$  decay, a realistic shell-model hamiltonian has been established in the  $sd$ -shell region; the so-called USD interaction[7]. The  $^{54}\text{Fe}$  and  $^{58}\text{Ni}$  nuclei belong to the middle  $pf$ -shell region. Though diagonalization of a hamiltonian in the full  $pf$ -shell is not yet possible for the middle  $pf$ -shell nuclei, a large-scale calculation in a loosely truncated space is successful to describe spectroscopic properties[8]. The  $k \leq 2$  configuration space, where  $k$  represents number of nucleons excited from  $0f_{7/2}$  to  $(0f_{5/2}1p_{3/2}1p_{1/2})$ , is adopted in this calculation, together with the Kuo-Brown hamiltonian[13]. The  $2\nu\beta\beta$  nuclear matrix-elements contain a product of a  $\text{GT}^+$  matrix-element from the initial state and a  $\text{GT}^-$  matrix-element from the final state. In the  $^{54}\text{Fe}$  and  $^{58}\text{Ni}$  decays, the  $k > 2$  configurations are forbidden in the intermediate  $\text{GT}^+$  state[14], as far as the initial state is restricted to the  $k \leq 2$  configurations. Notice that the lowest (*i.e.*,  $k = 0$ )

configuration shifts from the parent nucleus to the intermediate one, because the maximum number of nucleons which can occupy the  $0f_{7/2}$  orbit changes from nucleus to nucleus in this region. Unless a configuration has both the GT strengths from the initial and final states, this configuration does not contribute to the  $2\nu\beta\beta$  matrix-elements. Accordingly, only the  $k \leq 2$  configurations are relevant to the  $2\nu\beta\beta$  process, also in the  $\text{GT}^-$  strength from the final state. This situation is favorable because the  $k \leq 2$  wavefunctions have been inspected well by spectroscopic studies, including some single-GT transitions[14]. It should be stated here that these shell-model calculations in the  $sd$ - and  $pf$ -shell do not provide us with correct total binding energies. The Coulomb energy is neglected in the  $sd$ -shell hamiltonian, while the ground-state energy has been out of scope in the  $pf$ -shell calculation. We shift the energies of the intermediate states so as for the ground-state energy of the intermediate nuclei to fit to the experimental value, relative to the initial or final states. In the  $^{36}\text{Ar} \rightarrow ^{36}\text{S}$  and  $^{54}\text{Fe} \rightarrow ^{54}\text{Cr}$  decays the modes other than the EC/EC mode cannot occur because of the  $Q$ -values, while the  $\beta^+/\text{EC}$  mode has positive  $Q$ -value for  $^{58}\text{Ni} \rightarrow ^{58}\text{Fe}$ .

Though the practical application will be devoted to the  $\beta^+$  side, we here discuss how to calculate the  $2\nu\beta\beta$  nuclear matrix-elements more generally. The nuclear matrix-element of the  $2\nu\beta\beta$  process is written as

$$M_\omega(2\nu\beta\beta) = \sum_m \frac{\langle f || T(\text{GT}^\pm) || m \rangle \langle m || T(\text{GT}^\pm) || i \rangle}{E_m - E_i + \omega}, \quad (1)$$

where  $E_i$  and  $E_m$  denotes energies of the initial and intermediate nuclear states, respectively. The symbol  $\omega$  expresses energy of leptons emitted (or captured) during the step producing the intermediate state from the initial

state. Its value ranges from zero to the  $Q$ -value of the  $\beta\beta$  process. The initial state ( $|i\rangle$ ) is the ground state of the parent nucleus. In order for the  $\beta\beta$  decays to be detectable, a single-GT decay from the parent nucleus must be forbidden. This happens for some decays from even-even nuclei, owing to the pairing correlation. Hence the initial states of the  $\beta\beta$  decays have  $J^P = 0^+$ . The intermediate nuclear states ( $|m\rangle$ ), whose eigenenergy is denoted by  $E_m$ , should have  $J^P = 1^+$ . Although the final state ( $|f\rangle$ ) may have  $J^P = 2^+$  in some  $\beta\beta$  decays, the ground  $0^+$  state is expected to give the dominant branch[1]. In the practical applications to be discussed, the final states must be the ground state, because of the  $Q$ -values. The contribution of the Fermi-decay mode due to the isospin-mixing is known to be negligible[3], and is omitted in Eq.(1). The bare GT operator is given by

$$T^{\text{free}}(\text{GT}^\pm) = \sum_i g_A \sigma_i t_{\pm,i}, \quad (2)$$

where the summation runs over constituent nucleons and  $g_A = G_A/G_V = 1.26$ . It has been known that, however, effects of the core-polarization (CP) and meson-exchange currents (MEC) should be taken into account in shell-model calculations on the GT processes[15, 16]. For this reason we use effective GT operators,

$$T(\text{GT}^\pm) = T^{\text{free}}(\text{GT}^\pm) + \delta T(\text{GT}^\pm), \quad (3)$$

where

$$\delta T(\text{GT}^\pm) = \sum_i \left\{ \delta g_A(nl) \sigma_i + \delta g_{lA}(nl) l_i + \delta g_{pA}(nl, n'l') [Y^{(2)}(\hat{\mathbf{r}}_i) \sigma_i]^{(1)} \right\} t_{\pm,i}. \quad (4)$$

In the shell-model approach, the summation in Eqs.(2) and (4) is restricted to valence nucleons. The parameters  $\delta g_A$ ,  $\delta g_{lA}$  and  $\delta g_{pA}$  depend on  $n$  and  $l$ ; the quantum numbers of single-particle orbit which the  $i$ -th nucleon occupies. In the  $sd$ -shell region, an effective operator for the USD wavefunctions has been obtained[17], by making a global fitting of the single-particle parameters of Eq.(4) to the measured  $B(\text{GT})$  values. In the  $pf$ -shell region, we adopt the parameter-set evaluated by Towner from microscopic standpoints[15], which has been shown to yield a sound agreement with the data[14], combined with the  $k \leq 2$  Kuo-Brown wavefunctions.

Application of Eq.(1) associated with the above GT operators to the  $2\nu\beta\beta$  matrix-elements implicates the following two assumptions: (i) The contribution of high-lying intermediate states beyond the  $0\hbar\omega$  space is negligible, although a certain amount of the GT strength is carried out of the  $0\hbar\omega$  space due to the CP mechanism. This is expected because, in addition to large energy-denominator, the high-lying GT strengths from the initial and final states are unlikely to be coherent, and has been supported by a statistical estimate[18]. (ii) The two sequential GT transitions are separated so well that the intermediate nuclear states should be the nuclear energy-eigenstates. The time interval of the sequential GT transitions is ruled by the energy denominator via the uncertainty principle, leading to  $(1\text{--}10\text{MeV})^{-1}$ . It is much longer than the time-scale of the weak current, which is the inverse of the gauge-boson mass,  $\sim(10^2\text{GeV})^{-1}$ . The MEC process takes  $(10^2\text{MeV})^{-1}$  at most, owing to the pion mass. Because the MEC concern the  $\delta T(\text{GT})$  term, the correction due to the time of the meson propagation will not exceed a few percent of the total  $2\nu\beta\beta$  matrix-elements. Contribution of other higher-



order diagrams can be estimated to be negligibly small, in a similar manner. The assumption (ii) is thus plausible within a few percent accuracy.

The explicit construction of the intermediate energy-eigenstates ( $|m\rangle$ ) in Eq.(1) is difficult in most cases, even if the wavefunctions of the initial and final states are obtained. Although the method of solving a coupled linear equation[11] is less elaborate than full diagonalization of a hamiltonian, still it is not easy to obtain all the possible intermediate states. This is because there may be quite a large number of intermediate states. In the closure approximation adopted in earlier studies[3],  $E_m$  of Eq.(1) is replaced by a constant average value. We then have, assuming a  $0^+$  final state,

$$\begin{aligned} M_\omega(2\nu\beta\beta) &\sim \frac{1}{E_{\text{av}} - E_i + \omega} \sum_m \langle f || T(\text{GT}^\pm) || m \rangle \langle m || T(\text{GT}^\pm) || i \rangle \\ &= \frac{1}{E_{\text{av}} - E_i + \omega} \langle f || T(\text{GT}^\pm) \cdot T(\text{GT}^\pm) || i \rangle, \end{aligned} \quad (5)$$

and do not have to handle the intermediate states explicitly. The average energy  $E_{\text{av}}$  has been estimated mainly from the  $\text{GT}^\pm$  resonance energies. It has been recognized, both theoretically and experimentally, that this closure approach hardly gives reliable matrix elements. This indicates a problem in the estimate of  $E_{\text{av}}$  and/or in the procedure taking energy average itself.

However, averaging of energy is justified if we carry it out in a sufficiently small energy range. Let us consider a set of  $1^+$  states of the intermediate nucleus  $\{|\tilde{n}\rangle\}$  which exhausts the relevant  $\text{GT}^\pm$  strength from the initial state. The states  $|\tilde{n}\rangle$ 's do not have to be energy eigenstates. It is possible to insert  $\sum_n |\tilde{n}\rangle\langle\tilde{n}|$  into the numerator of Eq.(1),

$$M_\omega(2\nu\beta\beta) = \sum_{m,n} \frac{\langle f || T(\text{GT}^\pm) || m \rangle \langle m | \tilde{n} \rangle \langle \tilde{n} || T(\text{GT}^\pm) || i \rangle}{E_m - E_i + \omega}. \quad (6)$$

It should be commented that the set  $\{|\tilde{n}\rangle\}$  does not have to run out *all* the GT strength; it has only to exhaust the *relevant* strength. For instance, even if the GT strength has a certain isospin distribution, only the lowest isospin component needs to be considered for  $\{|\tilde{n}\rangle\}$ , because higher isospin components do not have GT-transition strength to  $|f\rangle$ . A state  $|\tilde{n}\rangle$  has large overlaps with some eigenstates and negligibly small ones with others. These overlaps depend on  $E_m$ . It is postulated that the energy distribution of  $|\tilde{n}\rangle$  is peaked so sharply that  $|m\rangle$ 's with large  $\langle m|\tilde{n}\rangle$  could have eigenenergies close to  $E_{\tilde{n}} \equiv \langle \tilde{n}|H|\tilde{n}\rangle$ . We then obtain, via the approximation  $E_m \simeq E_{\tilde{n}}$  under the presence of  $\langle m|\tilde{n}\rangle$ ,

$$M_\omega(2\nu\beta\beta) \simeq \sum_n \frac{1}{E_{\tilde{n}} - E_i + \omega} \sum_m \langle f||T(\text{GT}^\pm)||m\rangle \langle m|\tilde{n}\rangle \langle \tilde{n}||T(\text{GT}^\pm)||i\rangle. \quad (7)$$

The closure with respect to  $|m\rangle$  is available at this stage, giving

$$M_\omega(2\nu\beta\beta) \simeq \sum_n \frac{\langle f||T(\text{GT}^\pm)||\tilde{n}\rangle \langle \tilde{n}||T(\text{GT}^\pm)||i\rangle}{E_{\tilde{n}} - E_i + \omega}. \quad (8)$$

The state  $|\tilde{n}\rangle$  plays a role of a doorway state for a certain number of energy eigenstates  $|m\rangle$ . In comparison with Eq.(1), Eq.(8) appears simply an replacement of  $|m\rangle$  by  $|\tilde{n}\rangle$  and  $E_m$  by  $E_{\tilde{n}}$ . Namely, a good approximation will be obtained by using an appropriate set of doorway states instead of the intermediate energy-eigenstates. The approximation of Eq.(8) can be regarded as an extension of the closure approximation. It indeed reduces to a closure approximation when a single intermediate state (the GT state) is used for  $|\tilde{n}\rangle$ . The remaining problem is how to generate  $\{|\tilde{n}\rangle\}$  efficiently.

In Ref.[9], a cancellation mechanism has been shown by using a weakly-coupled two-configuration model. It is noted that this mechanism is comprehended in the above equations; the essential part of the argument in Ref.[9]

reappears if we regard  $|\tilde{n}\rangle$  as a state having a considerable  $\text{GT}^\pm$  strength from  $|i\rangle$  but no  $\text{GT}^\mp$  strength from  $|f\rangle$ . The vanishing  $\text{GT}^\mp$  strength prohibits  $|\tilde{n}\rangle$  from contributing to  $M_\omega(2\nu\beta\beta)$  (see Eq.(8)). There may be one or more states with opposite character, having a  $\text{GT}^\mp$  strength from  $|f\rangle$  but no  $\text{GT}^\pm$  strength from  $|i\rangle$ . Suppose that some of these states have energies close to  $E_{\tilde{n}}$ , and couple weakly to  $|\tilde{n}\rangle$ . This coupling gives rise to a certain fragmentation of  $|\tilde{n}\rangle$  over several eigenstates, which is here denoted by  $|m_1\rangle$ ,  $|m_2\rangle$ ,  $\dots$ ,  $|m_r\rangle$ . Their eigenenergies are close to  $E_{\tilde{n}}$ . Each of  $|m_1\rangle$ ,  $|m_2\rangle$ ,  $\dots$ ,  $|m_r\rangle$  may have a sizable contribution to  $M_\omega(2\nu\beta\beta)$ , because they have GT strengths both from  $|i\rangle$  and  $|f\rangle$ . These contributions, however, cancel one another, and the result obtained solely by  $|\tilde{n}\rangle$ , which gives the vanishing contribution to  $M_\omega(2\nu\beta\beta)$ , is recovered. The whole contribution of  $|m_1\rangle$ ,  $|m_2\rangle$ ,  $\dots$ ,  $|m_r\rangle$  to  $M_\omega(2\nu\beta\beta)$  is represented by  $|\tilde{n}\rangle$ , as is shown from Eq.(6) to (8) in more general cases.

The set  $\{|\tilde{n}\rangle\}$  has been assumed to exhaust the transition strength from the state  $|i\rangle$ , in the above discussion leading to Eq.(8). It should be noted that an analogous equation is derived by adopting a set of doorway states so as to exhaust the relevant GT strengths from  $|f\rangle$ . These two ways give the same value if they are convergent, although the speed of convergence may be different.

The present derivation of Eq.(8) discloses what conditions are required for  $\{|\tilde{n}\rangle\}$ . There are two conditions: (a) The set  $\{|\tilde{n}\rangle\}$  must exhaust the relevant GT strength either from the initial or final state, and (b) each doorway state  $|\tilde{n}\rangle$  has an energy distribution over  $|m\rangle$  with sharp peak around  $E_{\tilde{n}}$ , so as for  $E_m \simeq E_{\tilde{n}}$  in the energy denominator to be justified. A promising way to

obtain such approximate intermediate states has been proposed in Ref.[10], by applying Whitehead's moment method[12]. The algorithm is as follows:

- (I) Produce the state exhausting the relevant  $\text{GT}^\pm$  strength from the initial (final) state,  $|\text{GT}_{i(f)}^\pm\rangle \propto P_{\text{rel}} \cdot T(\text{GT}^\pm)|i(f)\rangle$ , where  $P_{\text{rel}}$  stands for a projection operator which picks up the relevant configurations.
- (II) Generate a set of bases by operating the shell-model hamiltonian  $H$  on  $|\text{GT}_{i(f)}^\pm\rangle$ ;  $H|\text{GT}_{i(f)}^\pm\rangle, H^2|\text{GT}_{i(f)}^\pm\rangle, \dots, H^N|\text{GT}_{i(f)}^\pm\rangle$ .
- (III) Diagonalize  $H$  within the space  $\Gamma^{(N)} \equiv \{|\text{GT}_{i(f)}^\pm\rangle, H|\text{GT}_{i(f)}^\pm\rangle, \dots, H^N|\text{GT}_{i(f)}^\pm\rangle\}$ . Each energy eigenvalue and eigenstate in this subspace are taken as  $E_{\tilde{n}}$  and  $|\tilde{n}\rangle$ .
- (IV) Increase  $N$ , until  $M_\omega(2\nu\beta\beta)$  converges.

Although the steps (II) and (III) are common with the Lanczos diagonalization procedure, the convergence of  $M_\omega(2\nu\beta\beta)$  does not necessarily imply the convergence about the intermediate states, as will be shown later. The condition (a) is obviously fulfilled, since  $\Gamma^{(N)}$  contains  $|\text{GT}_{i(f)}^\pm\rangle$ , into which all the relevant GT strength is concentrated. The simplest case of  $N = 1$  is equivalent to the closure approximation of Ref.[3]. Speed of the convergence for  $N$  depends on how well (b) is satisfied. This point will be examined below for the practical cases.

Since all the  $\beta\beta$  decays to be investigated belong to the  $\beta^+$  side, the present practical calculation has to do only with  $T(\text{GT}^+)$ , not  $T(\text{GT}^-)$ , in Eqs.(1—8). For the GT state generated from the initial or final state at the step (I),  $|\text{GT}_i^+\rangle$  or  $|\text{GT}_f^-\rangle$  is considered. When  $|\text{GT}_i^+\rangle$  is chosen at (I), we

do not use the  $P_{\text{rel}}$  operator (*i.e.*,  $P_{\text{rel}} = 1$ ). For  $|\text{GT}_f^- \rangle$ ,  $P_{\text{rel}}$  represents the isospin projection for the  $^{36}\text{Ar}$  decay, while for the  $^{54}\text{Fe}$  and  $^{58}\text{Ni}$  decays the projection onto the  $k \leq 2$  space is included as well.

Because of the phase space of the emitted leptons,  $\omega \sim Q/2$  yields a main contribution to the  $\beta\beta$  probabilities, where  $Q$  denotes the  $Q$ -value of the  $\beta\beta$  process. We examine convergence of the above method, by taking  $\omega = Q/2$  as a typical value of  $\omega$ . Fig.1 shows the convergence for  $N$  (the number of the iteration). The result on the EC/EC mode is presented for the  $^{58}\text{Ni}$  decay. The  $\beta^+$ /EC mode has no essential difference. The number of the  $J^P = 1^+, T = 1$  (*i.e.*, relevant) states with the  $sd$ -shell configuration is 54 in  $^{36}\text{Cl}$ , the intermediate product of the  $^{36}\text{Ar}$  decay. Hence a full diagonalization of the shell-model hamiltonian is possible. On the other hand, for  $^{54}\text{Mn}$  and  $^{58}\text{Co}$ , there are more than  $10^4$  states having  $J^P = 1^+$  and the lowest isospin, even in the present truncated configuration space. Nevertheless, the convergence is so rapid that  $N = 10$  could be almost sufficient for all these cases. This situation is quite similar to the  $^{48}\text{Ca}$  decay reported in Ref.[10]. The cases starting from the  $\text{GT}^+$  state and the  $\text{GT}^-$  state are compared for the  $^{36}\text{Ar}$  decay. We view that the  $\text{GT}^+$  case yields somewhat better convergence, though the difference is not quite big. The same holds for the  $^{54}\text{Fe}$  and  $^{58}\text{Ni}$  decays. The reason for this will be discussed later.

In Fig.2, the  $\text{GT}^+$  strengths from  $^{54}\text{Fe}$  are depicted for  $N = 10, 30$  and  $150$ . Obviously the strength function does not converge with  $N = 10$  and  $30$ . The convergence of the  $\text{GT}^-$  strength function is somewhat worse than the  $\text{GT}^+$  one. Nevertheless,  $M_\omega(2\nu\beta\beta)$  is convergent, as shown in Fig.1. This is because the condition (b) for the set  $\{|\tilde{n}\rangle\}$  is satisfied well, even with such a

Figure 1:

Figure 2:

small number for  $N$ . We can track how each strength for  $N = 10$  diffuses as  $N$  increases. For instance, about 90% of the GT<sup>+</sup> strength at  $E_x = 2.7\text{MeV}$  appearing in the  $N = 10$  case remains in  $E_x = 2.0\text{--}3.1\text{MeV}$  in the  $N = 150$  result. For the strengths with  $N = 30$ , about 90% of the  $E_x = 2.9\text{MeV}$  strength is shared only by the states at  $E_x = 2.7$  and  $3.1\text{MeV}$  of the  $N = 150$  result. In this manner, the  $N = 10$  or  $30$  strengths, particularly the low-lying ones, are found to stay in a small energy range around the original position. It is confirmed that the  $E_x \lesssim 5\text{MeV}$  strengths are convergent with  $N = 150$ , whereas higher-lying ones are not.

### 3 Dominance of low-lying states in intermediate nucleus

We next investigate, taking notice of the excitation energies, which intermediate states give significant contributions to the  $2\nu\beta\beta$  matrix-elements.

Fig.3 shows contribution of the intermediate  $1^+$  states to  $M_{\omega=Q/2}(2\nu\beta\beta)$ , as a function of the excitation energy. Summed value of the  $2\nu\beta\beta$  matrix-elements up to the excitation energy  $E_x$ ,

$$\sum_{n \text{ for } E_{\tilde{n}} - E_0 < E_x} \frac{\langle f || T(\text{GT}^\pm) || \tilde{n} \rangle \langle \tilde{n} || T(\text{GT}^\pm) || i \rangle}{E_{\tilde{n}} - E_i + \omega},$$

is displayed, in order to make the convergence for the energy transparent. The ground-state energy of the intermediate nucleus is denoted by  $E_0$  here. Thus the contribution of each intermediate state is presented by the stepwise increase or decrease. The result of the full diagonalization is shown for the  $^{36}\text{Ar}$  decay, while the  $N = 150$  results for the  $^{54}\text{Fe}$  and  $^{58}\text{Ni}$  decays. The computation of  $M_\omega(2\nu\beta\beta)$  begins with  $|\text{GT}_i^+\rangle$  at the step (I) (see Section 2). It is found that low-lying intermediate states dominate  $M_\omega(2\nu\beta\beta)$ . The  $E_x \lesssim 5\text{MeV}$  intermediate states govern  $M_\omega(2\nu\beta\beta)$  for the  $^{54}\text{Fe}$  and  $^{58}\text{Ni}$  cases, while a few of the  $5 < E_x \lesssim 10\text{MeV}$  states give a sizable contribution for  $^{36}\text{Ar}$ . This difference in energy might be caused by the difference in mass region. Furthermore, the number of the intermediate states giving considerable contribution to  $M_\omega(2\nu\beta\beta)$  is not very large. The dominance of a relatively small number of low-lying states in  $M_\omega(2\nu\beta\beta)$  seems consistent with the suggestion in Ref.[9] for the  $^{48}\text{Ca}$  decay, although the lowest  $1^+$  state is not enough to approximate  $M_\omega(2\nu\beta\beta)$  in the present cases.

Figure 3:

We shall look into the  $^{36}\text{Ar} \rightarrow ^{36}\text{S}$  case in more detail. The shell-model hamiltonian is fully diagonalized, without any further truncation in the  $sd$ -shell. The energy distribution of the contribution to the EC/EC nuclear matrix-element has been shown in Fig.3, being repeated in the middle sector of Fig.4. The upper (lower) sector of Fig.4 displays the energy distribution of the  $\text{GT}^+$  ( $\text{GT}^-$  with  $T = 1$ ) strength from the initial (final) state. The  $\text{GT}^+$  strength distribution correlates rather well to the steps of increase or decrease in the graph of  $M_\omega(2\nu\beta\beta)$ , though the size of the steps relative to the  $\text{GT}^+$  strengths comes smaller as the energy increases. The distribution of the  $T = 1$   $\text{GT}^-$  strength is quite different from that of  $\text{GT}^+$ , having greater weights in high-energy region. Indeed, the overlap between  $|\text{GT}_i^+\rangle$  and  $|\text{GT}_f^-\rangle$  is very small ( $\sim 2\%$ ). Higher-lying  $\text{GT}^-$  strengths hardly contribute to  $M_\omega(2\nu\beta\beta)$ , on account of the small overlap to the  $\text{GT}^+$  strength as well as of the large energy-denominator. Only a small portion (low-lying part) of the  $\text{GT}^-$  strength contributes to the  $2\nu\beta\beta$  matrix-element. This fact accounts for the slower convergence from  $|\text{GT}_f^-\rangle$  than from  $|\text{GT}_i^+\rangle$ . This mechanism applies also to the  $^{54}\text{Fe}$  and  $^{58}\text{Ni}$  decays.



Figure 4:

Contribution of the low-lying intermediate states is enhanced to a certain extent, due to the energy denominator. The effect of the energy denominator is, however, insufficient to account for the remarkable dominance of the low-lying states clarified presently. The particular significance of the low-lying GT strengths is qualitatively understood from a general argument on the shell structure of nuclei. To the first approximation, the initial and final states have configurations depicted by Fig.5-a) and b), because they are lowest-lying. The boxes in the graphs indicate the orbits occupied commonly between the initial and final states. The  $GT^+$  transition from the configuration of Fig.5-a) generates the configurations of Fig.5-c), while Fig.5-b) leads to Fig.5-d). The  $2\nu\beta\beta$  decay proceeds through the common configuration between Fig.5-c) and d). It is immediately found out that only the first graphs, which actually imply the low-energy part of the  $GT^+$  and  $GT^-$  strengths, are common between c) and d). Therefore, contribution of higher-lying GT strengths is hindered by the shell structure, as well as by the energy denominator. This shell effect is ignored in the closure approximation, making the energy denominator too large and giving rise to an underestimate of

Figure 5:

$M_\omega(2\nu\beta\beta)$ , as viewed in the  $N = 1$  limits of Fig.1. It is also noticed that, compared with the  $GT^+$  transition, the  $GT^-$  one has more patterns of high-lying configurations, originating in the neutron excess. The central energy of the  $GT^-$  strength is therefore higher than that of  $GT^+$ , as has been seen in Fig.4, even if we restrict ourselves to the lowest isospin component.

Let us consider the shell-structure effect on  $M_\omega(2\nu\beta\beta)$  more concretely, for the example of the  $^{36}\text{Ar}$  decay. The lowest configurations of  $^{36}\text{Ar}$  and  $^{36}\text{S}$  are

$$(p : 0d_{3/2}^{-2}, n : 0d_{3/2}^{-2}) \quad \text{for } ^{36}\text{Ar}, \quad (9)$$

$$(p : 0d_{3/2}^{-4}) \quad \text{for } ^{36}\text{S}, \quad (10)$$

on top of the  $^{40}\text{Ca}$  core. Thereby the  $GT^+$  excitation from  $^{36}\text{Ar}$  and the  $GT^-$  excitation from  $^{36}\text{S}$  primarily produce the following configurations of  $^{36}\text{Cl}$ ,

$$(p : 0d_{3/2}^{-3}, n : 0d_{3/2}^{-1}), \quad (p : 0d_{3/2}^{-2}0d_{5/2}^{-1}, n : 0d_{3/2}^{-1}) \quad \text{for } GT^+ \text{ from } ^{36}\text{Ar}, \quad (11)$$

$$(p : 0d_{3/2}^{-3}, n : 0d_{3/2}^{-1}), \quad (p : 0d_{3/2}^{-3}, n : 0d_{5/2}^{-1}) \quad \text{for } GT^- \text{ from } ^{36}\text{S}.$$

(12)

The common configuration  $(p : 0d_{3/2}^{-3}, n : 0d_{3/2}^{-1})$ , which is the lowest configuration of  $^{36}\text{Cl}$ , gives the main contribution to the  $2\nu\beta\beta$  matrix-element. The  $(p : 0d_{3/2}^{-3}, n : 0d_{3/2}^{-1})$  constitutes only a single  $1^+$  state with  $T = 1$ . This component is, however, fragmented in real situations, because other  $0\hbar\omega$  configurations appreciably mixes due to the residual interaction. Together with the leakage out of the configurations of Eqs.(9,10) for the initial and final states, this fragmentation of the  $1^+$  component distributes the  $2\nu\beta\beta$  matrix-elements over a certain range of energy. It is noted that the  $(p : 0d_{3/2}^{-3}, n : 0d_{5/2}^{-1})$  configuration yields higher energy than the  $(p : 0d_{3/2}^{-2}0d_{5/2}^{-1}, n : 0d_{3/2}^{-1})$  one, because the neutrons occupying  $0d_{5/2}$  are harder to be excited than the protons in the same orbit. In terms of the BCS theory, the quasiparticle energy of  $0d_{5/2}$  is higher for neutrons than for protons. Hence the  $\text{GT}^-$  energy should be substantially higher than the  $\text{GT}^+$  one.

In the  $^{54}\text{Fe}$  and  $^{58}\text{Ni}$  cases, the  $2\nu\beta\beta$  processes would be forbidden, if merely  $1p_{3/2}$  were active for neutrons. The principal contribution comes from the configurations with the excitation from  $1p_{3/2}$  to  $0f_{5/2}$ . It still holds that  $2\nu\beta\beta$  proceeds mainly through lower configurations of the intermediate nucleus. Thus the low-lying intermediate states dominate the  $2\nu\beta\beta$  matrix-elements, as shown in Fig.3.

We here mention a speciality of the  $^{48}\text{Ca} \rightarrow ^{48}\text{Ti}$  decay. To the first approximation,  $^{48}\text{Ca}$  can be regarded as a doubly magic core. The lowest configuration of  $^{48}\text{Ti}$  is  $(p : 0f_{7/2}^2, n : 0f_{7/2}^{-2})$ . The  $2\nu\beta\beta$  decay is mediated by the  $(p : 0f_{7/2}^1, n : 0f_{7/2}^{-1})$  configuration, which is the lowest configuration of

$^{48}\text{Sc}$ . This configuration allows a single  $1^+$  state, like the  $^{36}\text{Ar}$  case. On the other hand, the  $0f_{7/2}$  orbit is isolated and the residual interaction can hardly mix this configuration with other ones. Therefore it remains almost pure, constituting the lowest  $1^+$  state. This consideration accounts for the reason that the lowest  $1^+$  state already gives a good approximation to the total  $2\nu\beta\beta$  matrix-element in the  $^{48}\text{Ca}$  decay, as pointed out in Ref.[9], unlike the other cases investigated in this article. The dominance of the lowest  $1^+$  state has been suggested from experiments for the  $^{100}\text{Mo}$  decay[19], and an extensive study has been carried out also for several other decays[20]. This can also be explained by a similar argument for the nuclei with  $Z$  or  $N = 40 - 50$ , in which the isolation of the  $0g_{9/2}$  orbit plays an essential role. The  $^{128}\text{Te}$  and  $^{130}\text{Te}$  cases[19, 20] are a different matter. Another effect such as quadrupole deformation might be necessary to understand this case.

The role of the shell structure has not been recognized sufficiently so far. Despite the arguments for the  $^{48}\text{Ca}$  decay[9], there has been a lack of such discussions adapting to more general cases. In the  $0\nu\beta\beta$  decays, the difference of energy denominator among low- and high-lying intermediate states is much less important[1] than in  $2\nu\beta\beta$ . However, the shell-structure mechanism remains and lower-lying GT strengths will still be significant, because of a certain similarity of the  $0\nu\beta\beta$  nuclear matrix-elements to the  $2\nu\beta\beta$  ones.

The present calculation has been carried out with the algorithm developed in Ref.[10]. It has been confirmed extensively in this article how powerful this method is, by taking examples other than the  $^{48}\text{Ca}$  decay as well as by a detailed discussion. There are a few other minor differences of the present

study from that of Ref.[10]. While the GT operator proportional to  $\sigma t_{\pm}$  has been used in Ref.[10], more realistic GT operators are adopted here. This does not influence the speed of convergence, as expected. Although only the computation starting from  $|\text{GT}_i^-\rangle$  is considered in Ref.[10], we have tested both the  $|\text{GT}_i^+\rangle$  and  $|\text{GT}_f^-\rangle$  cases. A slight faster convergence of the  $|\text{GT}_i^+\rangle$  case has become evident. It is naturally expected in the  $\beta^-\beta^-$  decays that the calculation starting from  $|\text{GT}_f^+\rangle$  converges somewhat faster than from  $|\text{GT}_i^-\rangle$ .

The quasiparticle random-phase approximation (QRPA) has often been applied to calculating the  $\beta\beta$  nuclear matrix-elements. It is known, however, that results of the  $2\nu\beta\beta$  calculation with QRPA are seriously sensitive to  $g_{pp}$  around  $g_{pp} = 1$ [21, 22], where  $g_{pp}$  denotes a factor introduced for the particle-particle interaction. This problem regarding  $g_{pp}$  is crucial to predictability of the QRPA calculation. It has been shown in Ref.[22] that the low-lying GT spectra, particularly the  $\text{GT}^+$  ones, are sensitive to  $g_{pp}$ . Based on the above discussion of the shell-structure effect and the consequence of the present shell-model calculations, the  $g_{pp}$  problem in the  $2\nu\beta\beta$  calculation seems to originate primarily in the sensitivity of the low-lying  $\text{GT}^+$  strengths to  $g_{pp}$ .

It is emphasized that the low-lying GT strengths with  $E_x \lesssim (5\text{--}10)\text{MeV}$ , rather than higher-lying component such as the  $\text{GT}^-$ -resonance, are essential to the  $2\nu\beta\beta$  nuclear matrix-elements. There are several significant implications. As is well-known, energies and wavefunctions of lower-lying states converge rapidly in the Lanczos diagonalization algorithm. Convergence of the present algorithm is accelerated further by the dominance of the low-lying GT strengths, because its essential part is the same as the Lanczos

method. The low-lying GT strengths will provide us with a crucial test on reliability of the calculations of the  $2\nu\beta\beta$  nuclear matrix-elements. It is true also for the QRPA calculations. Both of the parent and daughter nuclei of the  $\beta\beta$  decays are stable against the single- $\beta$  decay. It is hopeful to measure by high-resolution charge-exchange experiments the low-lying GT strengths from the initial and final states. Theoretical approaches should be examined critically for the low-lying GT strengths by these measurements. As has been discussed in connection with Eq.(8), concise reproduction of individual GT strength is not necessarily required. It is requisite, however, to describe properly the average character of the low-lying strengths in a sufficiently small energy range. This point is more important than to reproduce the total GT strengths. Moreover, if we had a reliable assessment on the signs of the GT matrix-elements, the  $2\nu\beta\beta$  matrix-element could be obtained experimentally by using the measured GT strengths. In the present calculations and those for the  $^{48}\text{Ca}$  decay, energy regions adding positive and negative values to  $M_\omega(2\nu\beta\beta)$  appear nearly separated. It may not be difficult to learn the signs from realistic calculations.

## 4 Half-lives of $2\nu\beta\beta$ decays

The main purpose of this article is to clarify what is required to calculate the  $2\nu\beta\beta$  nuclear matrix-elements. As far as the calculated GT strengths from the initial and final states have not been examined sufficiently, we should not claim high precision for the  $2\nu\beta\beta$  matrix-elements calculated in the present study. We here show, however, the calculated half-lives, be-

cause there could be some interest in the prediction of the present realistic shell-model calculations. In order to evaluate half-lives of the  $2\nu\beta\beta$  decays, integration of the lepton degrees-of-freedom is carried out, by following Ref.[4]. As a result, half-lives of  $T_{1/2}^{2\nu}(\text{EC}/\text{EC}; {}^{36}\text{Ar} \rightarrow {}^{36}\text{S}) = 1.7 \times 10^{29}\text{yr}$ ,  $T_{1/2}^{2\nu}(\text{EC}/\text{EC}; {}^{54}\text{Fe} \rightarrow {}^{54}\text{Cr}) = 1.5 \times 10^{27}\text{yr}$  are obtained from the present nuclear matrix-elements. The half-lives of the  ${}^{58}\text{Ni}$  decay is shown in Table 1, in comparison with the QRPA results[6] and the data[23]. The present calculation gives half-lives somewhat longer, but comparable to those by the QRPA calculation. Both calculations predict much longer lifetimes than the lower-limits of experiments.

## 5 Summary

It has been discussed what conditions are demanded to compute the  $2\nu\beta\beta$  nuclear matrix-elements: We should prepare for a set of (approximate) intermediate states with (a) exhausting the relevant GT strength and (b) energy distribution having a sharp peak, over the energy eigenstates. An algorithm proposed in Ref.[10] based on Whitehead's moment method seems quite promising from this viewpoint, particularly when it is associated with large-scale realistic shell-model wavefunctions. This algorithm has been inspected, applied to the  ${}^{36}\text{Ar} \rightarrow {}^{36}\text{S}$ ,  ${}^{54}\text{Fe} \rightarrow {}^{54}\text{Cr}$  and  ${}^{58}\text{Ni} \rightarrow {}^{58}\text{Fe}$  decays. Quite rapid convergence has been shown. It has also been pointed out that the low-lying part of the intermediate GT strength dominates the  $2\nu\beta\beta$  rates, owing to the shell structure of nuclei as well as to the energy denominator. However, it will not be always true that only the lowest intermediate  $1^+$  state

is enough in evaluating the  $2\nu\beta\beta$  nuclear matrix-elements. It somewhat depends on the extent of the configuration mixing. Careful tests of the low-lying GT strengths, which will be doable with assistance of high-resolution charge-exchange experiments, are significant to predict the  $2\nu\beta\beta$  matrix-elements. Half-lives of those decays obtained within the present shell-model framework have been reported.

The authors are grateful to Dr. S. Cohen for careful reading of the manuscript. The numerical calculation is financially supported by Research Center for Nuclear Physics, Osaka University (Project No.95-A-01).

## References

- [1] M. Doi, T. Kotani and E. Takasugi, Prog. Theor. Phys. Suppl. **83**(1985)1.
- [2] H. Ejiri, Nucl. Phys. **A522**(1991)305c.
- [3] W. C. Haxton and G. J. Stephenson Jr., Prog. Part. Nucl. Phys. **12**(1984)409.
- [4] M. Doi and T. Kotani, Prog. Theor. Phys. **87**(1992)1207.
- [5] M. Doi and T. Kotani, Prog. Theor. Phys. **89**(1993)139.
- [6] M. Hirsch, K. Muto, T. Oda and H. V. Klapdor-Kleingrothaus, Z. Phys. **A347**(1994)151.



- [7] B. A. Brown and B. H. Wildenthal, *Ann. Rev. Nucl. Part. Sci.* **38**(1988)29.
- [8] H. Nakada, T. Sebe and T. Otsuka, *Nucl. Phys.* **A571**(1994)467.
- [9] L. Zhao, B. A. Brown and W. A. Richter, *Phys. Rev.* **C42**(1990)1120.
- [10] E. Caurier, A. Poves and A. P. Zuker, *Phys. Lett.* **B252**(1990)13.
- [11] K. Ogawa and H. Horie, *Nuclear Weak Processes and Nuclear Structure*, ed. M. Morita, H. Ejiri, H. Ohtsubo and T. Sato (World Scientific, Singapore, 1989), p.308.
- [12] R. R. Whitehead, *Moment Methods in Many Fermion Systems*, ed. B. J. Dalton, S. M. Grimes, J. D. Vary and S. A. Williams (Plenum, New York, 1980), p.235.
- [13] T. T. S. Kuo and G. E. Brown, *Nucl. Phys.* **A114**(1968)241.
- [14] H. Nakada and T. Sebe, *J. Phys.* **G**, in press.
- [15] I. S. Towner, *Phys. Rep.* **155**(1987)263.
- [16] A. Arima, K. Shimizu, W. Bentz and H. Hyuga, *Advances in Nuclear Physics*, ed. J. W. Negele and E. Vogt, vol.18. (Plenum, New York, 1988), p.1.
- [17] B. A. Brown and B. H. Wildenthal, *At. Data Nucl. Data Tables* **33**(1985)347.
- [18] M. Ericson, T. Ericson and P. Vogel, *Phys. Lett.* **B328**(1994)259.

- [19] J. Abad, A. Morales, R. Nunez-Lagos and P. F. Pacheo, *Ann. Fis.* **A80**(1984)9.
- [20] H. Ejiri and H. Toki, *J. Phys. Soc. Jpn.* **65**(1996)7.
- [21] O. Civitarese, A. Faessler and T. Tomoda, *Phys. Lett.* **B196**(1987)11.
- [22] K. Muto, E. Bender and H. V. Klapdor, *Z. Phys.* **A334**(1989)177, 187.
- [23] E. B. Norman and M. A. DeFaccio, *Phys. Lett.* **B148**(1984)31.

## Figure Captions

**Fig.1:** Convergence of  $M_{\omega=Q/2}(2\nu\beta\beta)$  for  $N$ . The upper sector shows the convergence starting from  $|\text{GT}_i^+\rangle$  for the three decays. In the lower sector, the convergence starting from  $|\text{GT}_i^+\rangle$  and that from  $|\text{GT}_f^-\rangle$  are compared for the  $^{36}\text{Ar}$  decay.

**Fig.2:**  $\text{GT}^+$  strength function for  $^{54}\text{Fe}$  calculated by Whitehead's moment method: the strength functions obtained with  $N = 10$  (upper), 30 (middle) and 150 (lower) are compared.

**Fig.3:**  $M_{\omega=Q/2}(2\nu\beta\beta)$  with contribution of the intermediate states up to the excitation energy specified by the horizontal axis.

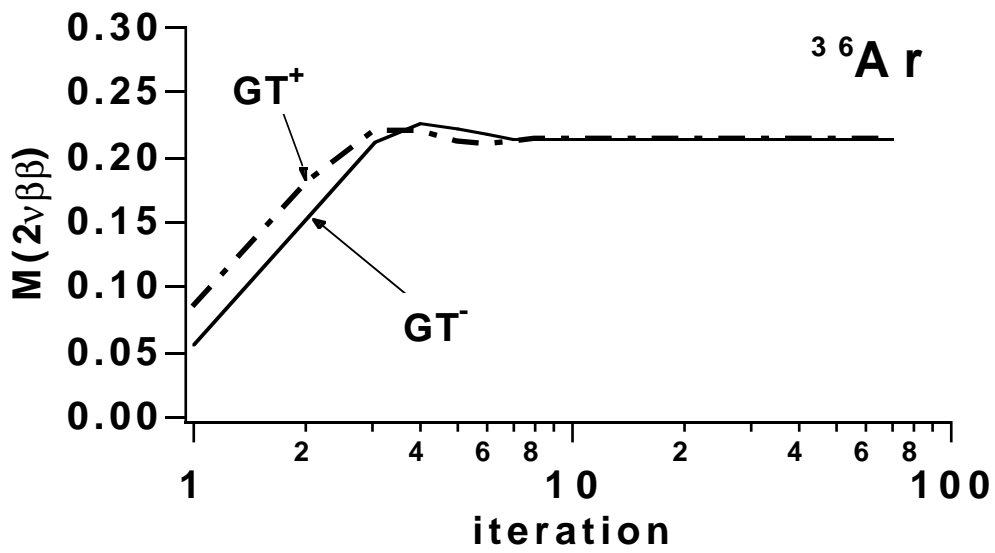
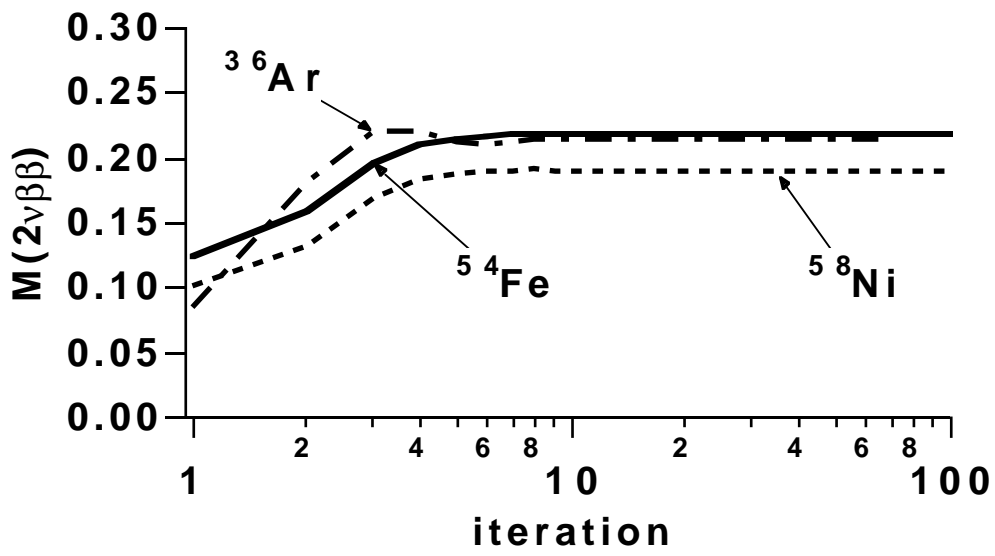
**Fig.4:**  $\text{GT}^+$  strength function of  $^{36}\text{Ar}$  (upper),  $\text{GT}^-$  strength function of  $^{36}\text{S}$  (lower) and  $M_{\omega=Q/2}(2\nu\beta\beta)$  up to  $E_x$  for the  $^{36}\text{Ar}$  decay (middle).

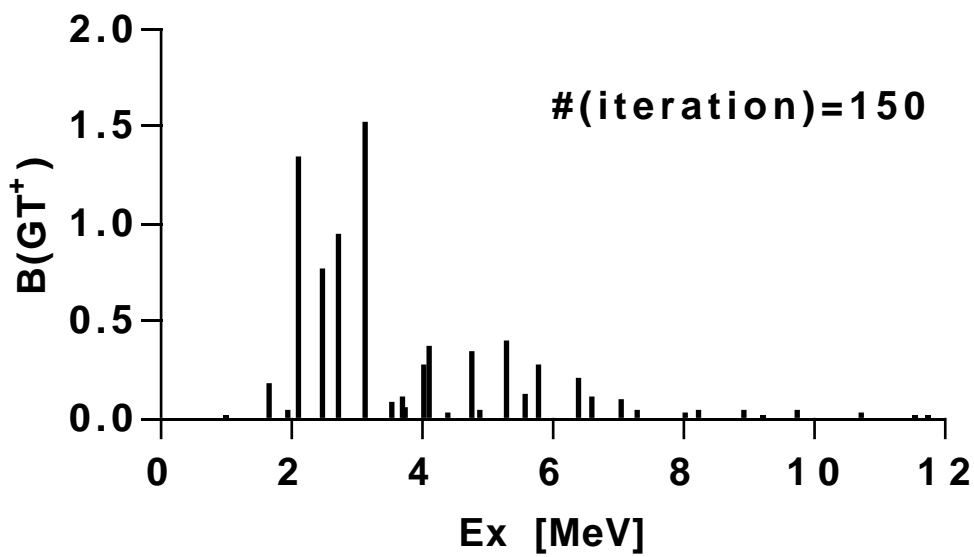
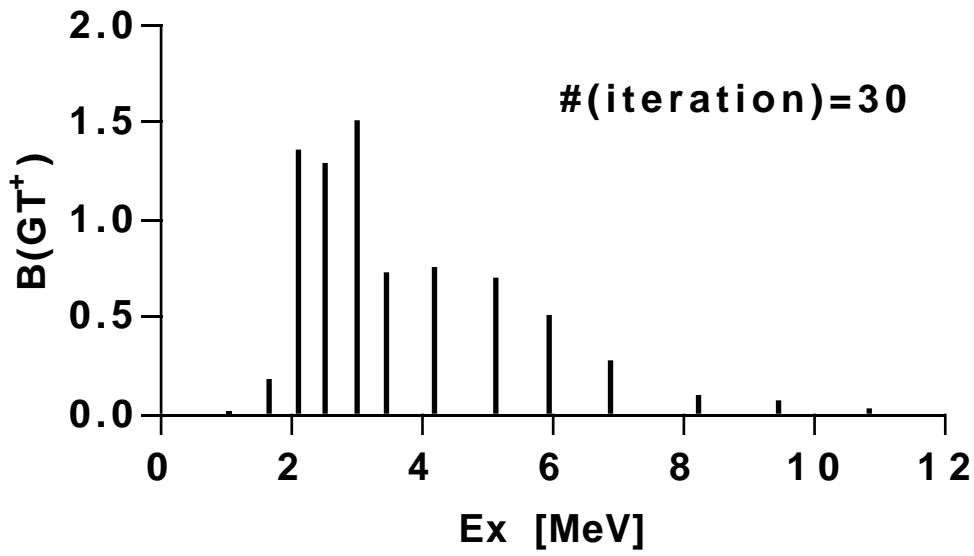
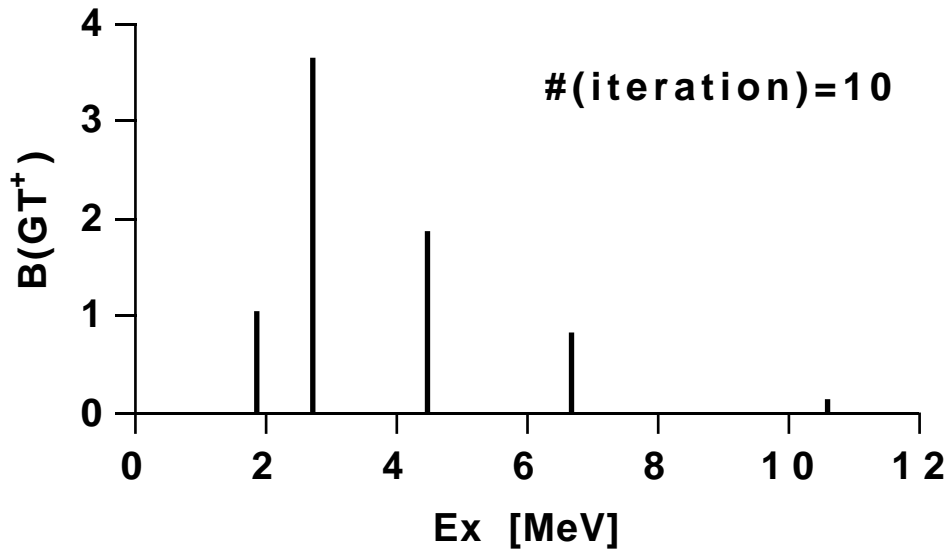
**Fig.5:** Proton and neutron schematic configurations regarding the  $\beta\beta$  decay.  
a,b): Ground-state configurations of the initial and final nuclei.  
c) Possible configurations generated by the  $\text{GT}^+$  transition from the state of a).  
d) Possible configurations generated by the  $\text{GT}^-$  transition from the state of b).

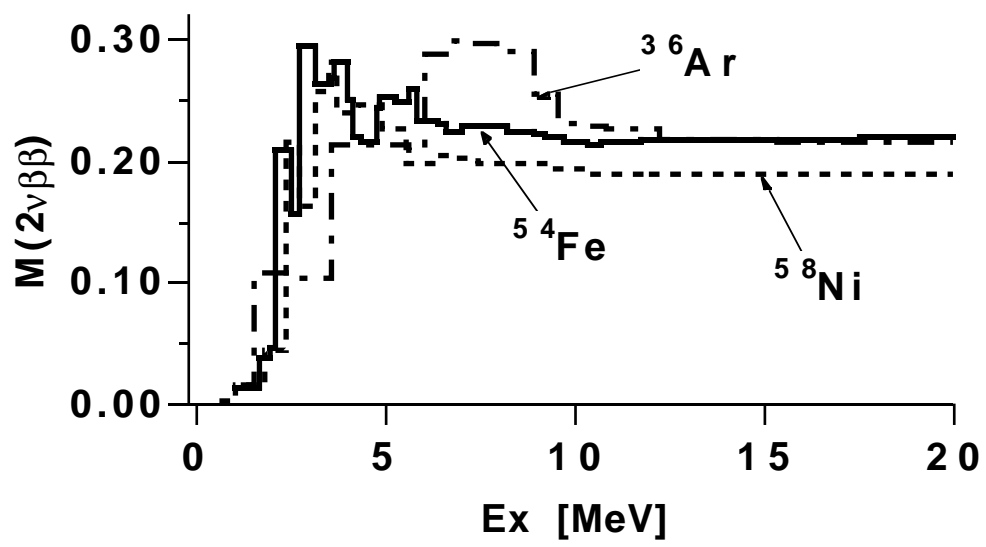
## Tables

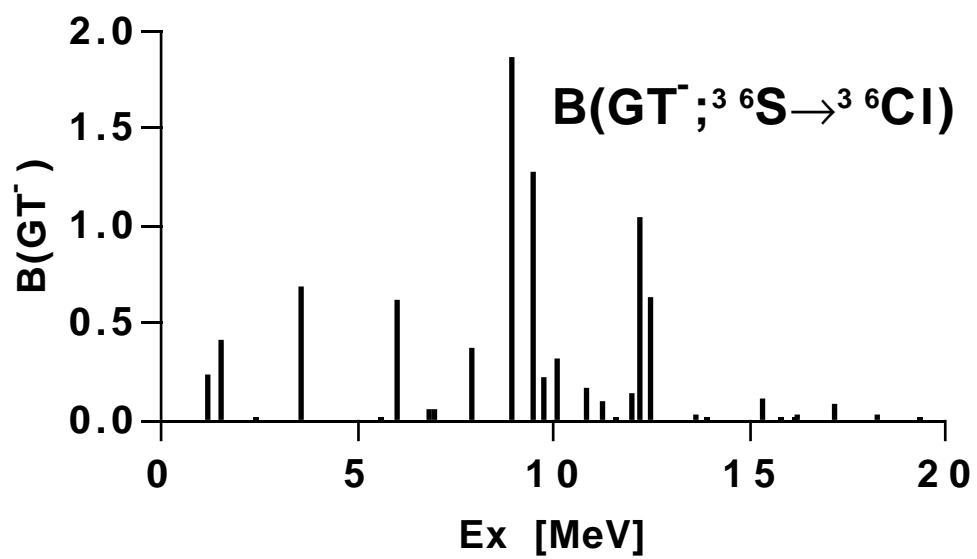
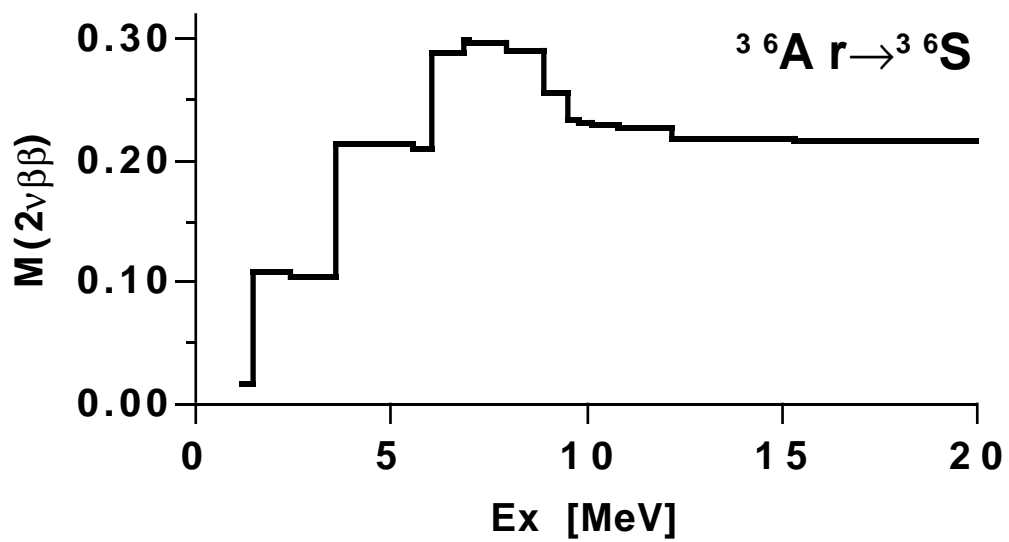
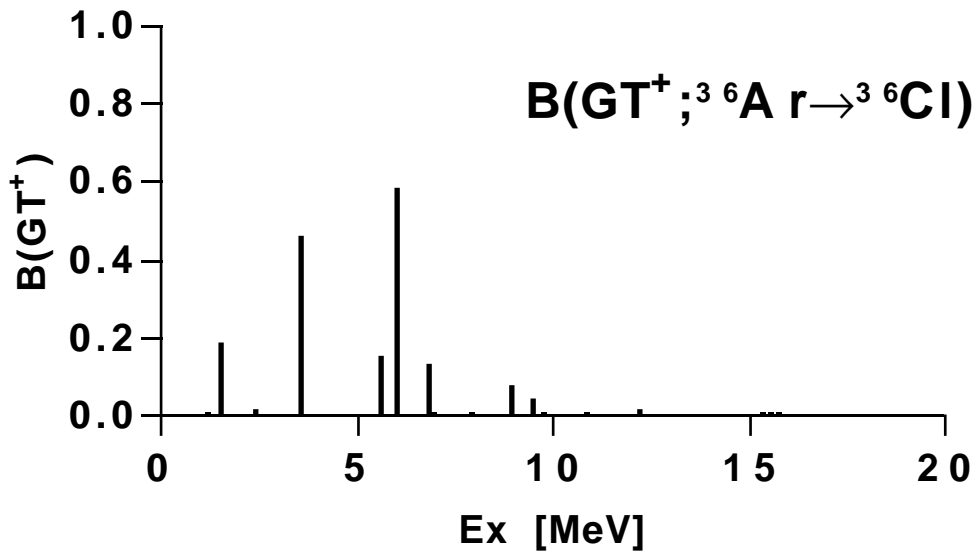
Table 1: Half-lives (yr) of the  $^{58}\text{Ni} \rightarrow ^{58}\text{Fe}$  decay. The values obtained in the present calculation are compared with those of the QRPA calculation of Ref.[6] and of the experimental lower-limits[23].

	Present work	QRPA	Exp.
EC/EC	$6.1 \times 10^{24}$	$3.9 \times 10^{24}$	$> 2.1 \times 10^{19}$
$\beta^+$ /EC	$8.6 \times 10^{25}$	$5.5 \times 10^{25}$	$> 6.2 \times 10^{19}$



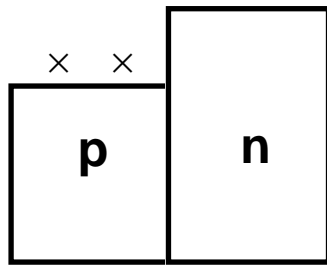




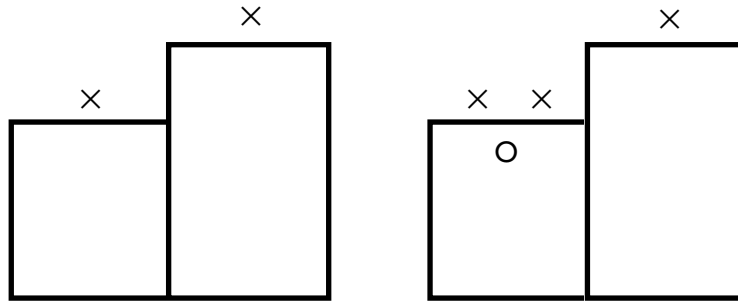




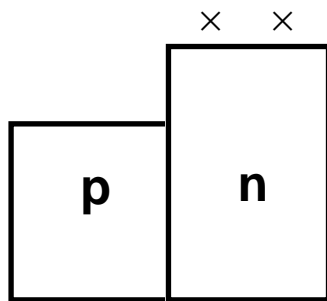
**a)**



**c)**



**b)**



**d)**

